



Thickness and density measurements in biofilm with a fiber optic sensor  
by Gabriele Sabine Walser

A thesis submitted in partial fulfillment of the requirements for the degree of Master of Science in  
Environmental Engineering  
Montana State University  
© Copyright by Gabriele Sabine Walser (1990)

Abstract:

The purpose of this study was to measure biofilm thickness and density using a fiber optic sensor.  
Biofilm thickness was related to shear stress.

Biofilm was grown in a horizontal rotating disk reactor under laminar flow conditions. Measurements  
of biofilm thickness and density were performed with an intensity modulated fiber optic sensor.

The biofilm-water interface and the substratum-biofilm interface were detected with the sensor and the  
biofilm thickness was determined. The sensor was calibrated to measure biofilm density. The results  
for biofilm grown in the rotating disk reactor indicate that biofilm thickness depends on shear stress.  
The maximum biofilm thickness was found for a shear stress of approximately  $0.08 \text{ Nm}^{-2}$ . Biofilm  
thickness decreases for higher and lower shear stresses.

THICKNESS AND DENSITY MEASUREMENTS IN BIOFILM  
WITH A FIBER OPTIC SENSOR

by

Gabriele Sabine Walser

A thesis submitted in partial fulfillment  
of the requirements for the degree

of

Master of Science

in

Environmental Engineering

MONTANA STATE UNIVERSITY  
Bozeman, Montana

July 1990

N378  
W1678

APPROVAL

of a thesis submitted by

Gabriele Sabine Walser

This thesis has been read by each member of the thesis committee and has been found to be satisfactory regarding content, English usage, format, citations, bibliographic style, and consistency, and is ready for submission to the College of Graduate Studies.

July 16, 1990  
Date

John J. Nowakowski  
Chairperson, Graduate Committee

Approved for the Major Department

16 July '90  
Date

Madeline E. Long  
Head, Major Department

Approved for the College of Graduate Studies

July 25, 1990  
Date

Henry J. Parsons  
Graduate Dean

## STATEMENT OF PERMISSION TO USE

In presenting this thesis in partial fulfillment of the requirements for a master's degree at Montana State University, I agree that the Library shall make it available to borrowers under rules of the Library. Brief quotations from this thesis are allowable without special permission, provided that accurate acknowledgement of source is made.

Permission for extensive quotation from or reproduction of this thesis may be granted by my major professor, or in his absence, by the Dean of Libraries when, in the opinion of either, the proposed use of the material is for scholarly purposes. Any copying or use of the material in this thesis for financial gain shall not be allowed without my written permission.

Signature

Harvie Walser

Date

July 16, 1990

## ACKNOWLEDGEMENTS

I wish to express my appreciation to the following:

Zbigniew Lewandowski for his guidance in the experimental work of this thesis which made my work productive and enjoyable.

Warren Jones for his advice, support and encouragement and Bill Characklis for his advice and comments throughout my work.

The whole "IPA gang", Vivek, Robert, Brent, Ewout, Bill, Feisal, Whon Chee, Satoshi and Bryan, for being such a fun group to work with.

Paul and Ann, for always being ready to help and answer questions.

Wendy, Diane, Lynda, Jamie, Susan, Mary, Frank, Al, and Dick for their support.

## TABLE OF CONTENTS

	Page
APPROVAL .....	ii
STATEMENT OF PERMISSION TO USE .....	iii
ACKNOWLEDGEMENTS .....	iv
TABLE OF CONTENTS .....	v
LIST OF TABLES .....	vii
LIST OF FIGURES .....	viii
ABSTRACT .....	xiii
INTRODUCTION .....	1
Goal of Research .....	2
Objectives of Research .....	2
BACKGROUND .....	3
Models for the Influence of Shear Stress on Biofilm Accumulation .....	3
The Influence of Shear Stress on Biofilm Thickness and Density .....	5
Shear Stress on a Rotating Disk .....	7
Fiberoptic Sensors in Biofilm Research .....	9
MATERIALS AND METHODS .....	18
The Rotating Disk Reactor .....	18
The Fiber Optic Sensing Device .....	20
Procedures .....	22
RESULTS .....	25
Location of the Biofilm-Water Interface .....	25
Biofilm Thickness .....	29
Biofilm Density .....	32
Biofilm Thickness and Extinction Coefficient versus Shear Stress .....	35

TABLE OF CONTENTS-Continued

	Page
DISCUSSION .....	39
Fiber Optic Sensor Construction and Application .....	39
The Delineation of the Biofilm and the Water Phase .....	40
The Determination of the Biofilm Thickness .....	41
The Determination of the Biofilm Density .....	43
The Relation between Biofilm Thickness, Density and Shear Stress .....	45
CONCLUSIONS .....	47
REFERENCES CITED .....	48
NOMENCLATURE .....	51
APPENDICES	
A. The Calibration of the Micromanipulator .....	55
B. The Variation of Absorbance with Distance to the Substratum for Density Calibration .....	57
C. The Variation of Absorbance with Distance to the Substratum for 4-Day-Old Biofilm .....	62
D. The Variation of Absorbance with Distance to the Substratum for 7-Day-Old Biofilm .....	81
E. The Variation of Absorbance with Distance to the Substratum for Biofilm Grown under Non-Laminar Flow Conditions .....	94
F. Light Intensity Measurement in Water .....	108

## LIST OF TABLES

Table		Page
1.	Literature data about the influence of shear stress on biofilm thickness .....	6
2.	Comparison of volumetric measured density with optically measured density .....	33
3.	Step length versus micromanipulator settings .....	56
4.	Step frequency for different micromanipulator settings .....	56

## LIST OF FIGURES

Figure	Page
1. Biofilm schematic .....	3
2. Velocity profile for Couette-flow .....	9
3. A sensing device in general form and in the form used for the fiber optic sensor .....	11
4. Schematic of an intensity-modulated sensing device .....	11
5. Path of a ray through a fiber optic cable .....	14
6. Bending effects on critical angle .....	15
7. Frequency modulation with a sinusoidal modulating wave .....	16
8. Photograph of the rotating disk reactor .....	19
9. Schematic diagram of measurement device setup .....	21
10. Enlarged picture of the fiber optic sensor tip .....	22
11. The variation of light intensity with distance from the substratum .....	26
12. The variation of light intensity with distance from the substratum .....	27
13. The variation of light intensity with distance from the substratum .....	28
14. The variation in light intensity with distance from the substratum .....	30
15. The variation in light intensity with distance from the substratum .....	31
16. Absorbance of homogenized biofilm versus biomass concentration ("biofilm density" ) measured with a spectrophotometer at 660 nm .....	32
17. Absorbance in a biofilm versus distance .....	34
18. Biofilm thickness versus shear stress/velocity for a 4-day-old biofilm .....	36

LIST OF FIGURES-Continued

Figure	Page
19. Biofilm thickness versus shear stress/velocity for a 7-day-old biofilm . . . . .	37
20. Biofilm thickness vs. flow velocity for a biofilm grown under non-laminar flow conditions . . . . .	37
21. Extinction coefficient versus shear stress for a 7-day-old biofilm grown under laminar flow conditions . . . . .	38
22. The variation of light intensity with distance from the substratum in a fluffy or diffuse biofilm . . . . .	42
23. Biofilm with distinct base and surface film . . . . .	45
24. Absorbance measurements in biofilm sample A . . . . .	58
25. Absorbance measurements in biofilm sample B . . . . .	60
26. Absorbance measurements in 6 cm distance from the center of the disk . . . . .	63
27. Absorbance measurements in 7 cm distance from the center of the disk . . . . .	64
28. Absorbance measurements in 8 cm distance from the center of the disk . . . . .	65
29. Absorbance measurements in 9 cm distance from the center of the disk . . . . .	66
30. Absorbance measurements in 11 cm distance from the center of the disk . . . . .	67
31. Absorbance measurements in 12 cm distance from the center of the disk . . . . .	68
32. Absorbance measurements in 13 cm distance from the center of the disk . . . . .	69
33. Absorbance measurements in 14 cm distance from the center of the disk . . . . .	70

## LIST OF FIGURES-Continued

Figure	Page
34. Absorbance measurements in 16 cm distance from the center of the disk .....	71
35. Absorbance measurements in 17 cm distance from the center of the disk .....	72
36. Absorbance measurements in 18 cm distance from the center of the disk .....	73
37. Absorbance measurements in 21 cm distance from the center of the disk .....	74
38. Absorbance measurements in 23 cm distance from the center of the disk .....	75
39. Absorbance measurements in 24 cm distance from the center of the disk .....	76
40. Absorbance measurements in 26 cm distance from the center of the disk .....	77
41. Absorbance measurements in 27 cm distance from the center of the disk .....	78
42. Absorbance measurements in 28 cm distance from the center of the disk .....	79
43. Absorbance measurements in 29 cm distance from the center of the disk .....	80
44. Absorbance measurements in 11 cm distance from the center of the disk .....	82
45. Absorbance measurements in 16 cm distance from the center of the disk .....	83
46. Absorbance measurements in 17 cm distance from the center of the disk .....	84
47. Absorbance measurements in 18 cm distance from the center of the disk .....	85

LIST OF FIGURES-Continued

Figure	Page
48. Absorbance measurements in 19 cm distance from the center of the disk .....	86
49. Absorbance measurements in 21 cm distance from the center of the disk .....	87
50. Absorbance measurements in 22 cm distance from the center of the disk .....	88
51. Absorbance measurements in 23 cm distance from the center of the disk .....	89
52. Absorbance measurements in 24 cm distance from the center of the disk .....	90
53. Absorbance measurements in 26 cm distance from the center of the disk .....	91
54. Absorbance measurements in 27 cm distance from the center of the disk .....	92
55. Absorbance measurements in 28 cm distance from the center of the disk .....	93
56. Absorbance measurements in 7 cm distance from the center of the disk .....	95
57. Absorbance measurements in 11 cm distance from the center of the disk .....	96
58. Absorbance measurements in 12 cm distance from the center of the disk .....	97
59. Absorbance measurements in 13 cm distance from the center of the disk .....	98
60. Absorbance measurements in 14 cm distance from the center of the disk .....	99
61. Absorbance measurements in 16 cm distance from the center of the disk .....	100

LIST OF FIGURES-Continued

Figure	Page
62. Absorbance measurements in 17 cm distance from the center of the disk .....	101
63. Absorbance measurements in 18 cm distance from the center of the disk .....	102
64. Absorbance measurements in 19 cm distance from the center of the disk .....	103
65. Absorbance measurements in 21 cm distance from the center of the disk .....	104
66. Absorbance measurements in 22 cm distance from the center of the disk .....	105
67. Absorbance measurements in 24 cm distance from the center of the disk .....	106
68. Absorbance measurements in 26 cm distance from the center of the disk .....	107
69. Light intensity measurement in water .....	109

## ABSTRACT

The purpose of this study was to measure biofilm thickness and density using a fiber optic sensor. Biofilm thickness was related to shear stress.

Biofilm was grown in a horizontal rotating disk reactor under laminar flow conditions. Measurements of biofilm thickness and density were performed with an intensity modulated fiber optic sensor.

The biofilm-water interface and the substratum-biofilm interface were detected with the sensor and the biofilm thickness was determined. The sensor was calibrated to measure biofilm density. The results for biofilm grown in the rotating disk reactor indicate that biofilm thickness depends on shear stress. The maximum biofilm thickness was found for a shear stress of approximately  $0.08 \text{ Nm}^{-2}$ . Biofilm thickness decreases for higher and lower shear stresses.

## INTRODUCTION

Inert surfaces immersed in water become colonized with microorganisms forming biofilms. Biofilms are undesirable in drinking water systems, where they pose a threat to the hygienic safety, as well as they are undesirable in industrial water systems, where biofilms deteriorate the quality of the product. Biofilm also obstruct the heat transfer in cooling towers. Conversely, biofilms are desirable in many biotechnological applications where microbial cells are preferred fixed to a substratum in order to resist washout. With growing interest in the role of biofilms, a growing interest in the modeling of biofilm systems has been reported (Grady, 1982). New models have to be verified by testing their variables in experiments. Biofilm thickness and density are variables used in most models, therefore experimental methods must be found to determine thickness and density. If thickness and density can be measured, they can be related to other parameters in the model, as was done in this thesis where a correlation between biofilm thickness and shear stress was found. A measurement system based on fiber optics was chosen because fiber optic sensors have several advantages over other sensors. They are durable and immune from electromagnetic interference and the small size of the fiber optic sensor makes it especially attractive for measurements in biofilm.

### Goal of Research

The goal of the research was to measure thickness and optical density of biofilms using a fiber optic sensor.

### Objectives of Research

The specific objectives of the research related to sensor application to measure biofilm thickness and density were as follows:

1. Determine the position of the biofilm-water interface using a fiber optics sensor.
2. Measure the biofilm thickness using a fiber optic sensor.
3. Determine the extinction coefficient of the biofilm.
4. Measure the density of the biofilm.
5. Correlate biofilm thickness, extinction coefficient and density to shear stress in a rotating disc reactor.

## BACKGROUND

Models for the Influence of Shear Stress  
on Biofilm Accumulation

Biofilm accumulates on surfaces immersed in water. It is assumed that biofilm consists of one or more homogeneous layers of biomass (Figure 1).

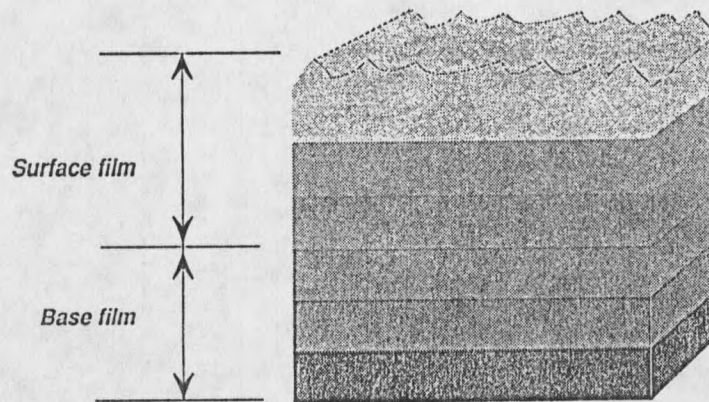


Figure 1. Biofilm schematic. The density of the biomass changes throughout the biofilm.

A numerical model for the prediction of biofilm accumulation and activity has been developed (Characklis et al., 1988). The model predicts biofilm accumulation as the net result of several physical, chemical and microbiological processes. A biofilm material balance encompasses growth, attachment and detachment, as shown in equation (1):

$$\text{accumulation} = \text{growth} + \text{attachment} - \text{detachment} \quad (1)$$

Detachment consists of erosion and sloughing. Sloughing occurs when large areas of biofilm detach from the wall. Sloughing usually removes all the biofilm down to

the substratum. Detached pieces of biofilm are removed by the flow of the bulk liquid. Erosion is the constant removal of single cells or a small group of cells from the biofilm, and is largely attributed to shear stress at the biofilm-fluid interface. Erosion rate has been expressed through the following formula (Characklis et al., 1988):

$$R_e = k_e \sigma \rho_f A L \quad (2)$$

where  $R_e$  is the erosion rate,  $k_e$  the erosion coefficient,  $\sigma$  the shear stress,  $\rho_f$  the film density,  $A$  the surface area of the biofilm and  $L$  the biofilm thickness. The erosion coefficient can be determined if a correlation between the biofilm thickness and the shear stress is established.

Rittmann (1982) developed an expression for detachment which encompasses erosion and sloughing. Since detachment of biofilm is a surface phenomenon, the rate of detachment,  $R_d$ , is defined as a surface rate:

$$R_d = b_d X_b L \quad (3)$$

where  $b_d$  is the surface detachment coefficient,  $X_b$  the biofilm density and  $L$  the biofilm thickness.

The detachment coefficient,  $b_d$ , can be expressed as a function of shear stress. Different expressions for the relation between shear stress and detachment coefficient could be found, depending on the biofilm thickness and biofilm roughness. Other factors might also influence the relation.

For a biofilm thinner than  $30\mu\text{m}$  the following expression could be found (Rittmann, 1989):

$$b_d = 3.62 * 10^{-6} \sigma^{0.58} \quad (4)$$

For thicker biofilms the following equation held true:

$$b_d = 3.62 * 10^{-6} \{ \sigma / [1 + 0.0443(L-30)] \}^{0.58} \quad (5)$$

The Influence of Shear Stress  
on Biofilm Thickness and Density

Erosion controls the extent of biofilm accumulation and thus determines the biofilm thickness. As shown in the models above, erosion is controlled by shear stress. Most previous experiments, however, investigated the influence of flow velocity on biofilm accumulation (Table 1). While flow velocity and shear stress are related through the system geometry, it is the shear stress that directly affects the development of the biofilm.

Kornegay and Andrews (1967) measured biofilm thickness versus shear stress. They found a strong decline in the biofilm thickness when the shear stress was increased from 1 to 3  $\text{Nm}^{-2}$ . In a study of biofilm accumulation in turbulent flow, Characklis (1980) found that biofilm thickness is dependent on shear stress and glucose loading rate. The dependence of biofilm thickness on shear stress is smaller for lower substrate loading rates. Only a small decrease in biofilm thickness was found for an increase in shear stress from 2 to 3  $\text{Nm}^{-2}$ , when the substrate loading rate was low.

Zelver et al. (1982) did not find a significant difference in biofilm accumulation between fluid velocities of 0.30  $\text{ms}^{-1}$  and 0.50  $\text{ms}^{-1}$ . Harty and Bott (1981) measured the effect of increasing velocity on maximum biofilm thickness on a simulated heat exchanger surface. Their results showed that an increase in velocity of 450% from 0.1  $\text{ms}^{-1}$  to 0.55  $\text{ms}^{-1}$  caused a decrease in the maximum biofilm thickness of 90%. A similar reduction was found for the accumulation rate. Bland et al. (1978) evaluated the accumulation of slime in drainage pipes. Up to 0.7 kg dry matter  $\text{m}^{-2}$  was deposited in pipes close to a turbulent inlet at a velocity of 0.5  $\text{ms}^{-1}$ , whereas at a velocity of 2.4  $\text{ms}^{-1}$ , deposition was seldom greater than 0.05 kg  $\text{m}^{-2}$ . Conversely, Pedersen (1982b) observed a significant

increase in rate of biofilm accumulation in seawater when the water velocity was increased from  $0.005 \text{ ms}^{-1}$  to  $0.15 \text{ ms}^{-1}$ . At these low velocities, biofilm accumulation is probably mass-transfer-limited for the substrate, and an increase in velocity should increase the biofouling rate.

Table 1. Literature data about the influence of shear stress on biofilm thickness.

Reference	Experimental condition	System variable	Parameter measured	Results
Kornegay and Andrews, 1967	RotoTorque turbulent flow	shear stress $1 - 3 \text{ Nm}^{-2}$	biofilm thickness	shear stress $\uparrow$ thickness $\downarrow$
Characklis, 1980	RotoTorque turbulent flow	shear stress $2-3 \text{ Nm}^{-2}$ glucose loading	biofilm thickness	shear stress $\uparrow$ thickness $\downarrow$
Zelver et al., 1982	tube reactor turbulent flow	fluid velocity $0.3 - 0.5 \text{ ms}^{-1}$	accumulation rate	velocity $\uparrow$ rate = const.
Harty and Bott, 1981	plug flow reactor turbulent flow	fluid velocity $0.1 - 0.55 \text{ ms}^{-1}$	maximum thickness	velocity $\uparrow$ thickness $\downarrow$
Bland et al., 1978	drainage pipes turbulent flow	fluid velocity $0.5 - 2.4 \text{ ms}^{-1}$	acc. solids dry mass	velocity $\uparrow$ dry mass $\downarrow$
Pedersen, 1982b	square cell; lamellar glass laminar flow	fluid velocity $0.005 - 0.15 \text{ ms}^{-1}$	accumulation rate	velocity $\uparrow$ rate $\uparrow$

While not studied as extensively as the relationship between thickness and shear stress, biofilm density is also influenced by shear stress. Characklis (1980) investigated the influence of shear stress on biofilm density. An increase of biofilm density with an increase in shear stress was observed. Kornegay and Andrews (1967) conducted

experiments in a RotoTorque reactor under different shear stresses. Increasing shear stress had no significant influence on biofilm density under high substrate loading rates.

### Shear Stress on a Rotating Disk

One of the objectives of this thesis was to correlate biofilm thickness to shear stress; thus, an experimental system was needed in which the shear stress could be calculated precisely. A reactor in which the disk revolves in a very tight housing under laminar flow conditions meets this condition.

For laminar flow the Reynolds number,  $Re$ , has to be smaller than  $10^5$ . The Reynolds number can be calculated in the following manner:

$$Re = R^2\omega/\nu \quad (6)$$

where  $R$  is the radius of the disk,  $\theta$  the radial velocity and  $\nu$  the kinematic viscosity.

The width of the gap between the rotating disk and the housing,  $s$ , has to be smaller than the boundary layer,  $b$ . The boundary layer thickness can be calculated from velocity and continuity equations for a disk in an infinite water bath.

We state that all velocities are independent of the angular coordinate,  $\theta$ , for reasons of symmetry. The following velocity equations and continuity equations then hold true (von Kármán, 1921):

$$v_r \frac{\delta v_r}{\delta r} + v_z \frac{\delta v_x}{\delta x} - \frac{v_r^2}{r} = -\frac{1}{\rho} \frac{\delta p}{\delta r} + \nu \left( \frac{\delta^2 v_r}{\delta r^2} + \frac{\delta}{\delta r} \left( \frac{v_r}{r} \right) + \frac{\delta^2 v_r}{\delta x^2} \right) \quad (7)$$

$$v_r \frac{\delta v_t}{\delta r} + v_x \frac{\delta v_x}{\delta x} - \frac{2v_t v_r}{r} = \nu \left( \frac{\delta^2 v_t}{\delta r^2} + \frac{3\delta}{r} \frac{v_t}{\delta r} + \frac{\delta^2 v_t}{\delta x^2} \right) \quad (8)$$

$$v_r \frac{\delta v_x}{\delta r} + v_x \frac{\delta v_x}{\delta x} = -\frac{1}{\rho} \frac{\delta p}{\delta x} + \nu \left( \frac{\delta^2 v_x}{\delta r^2} + \frac{1}{r} \frac{\delta v_x}{\delta r} + \frac{\delta^2 v_x}{\delta x^2} \right) \quad (9)$$

$$\frac{\delta V_r}{\delta r} + \frac{V_r}{r} + \frac{\delta V_x}{\delta x} = 0 \quad (10)$$

The system can be solved with the following functions:

$$v_r = r f(x) \quad v_t = r g(x) \quad v_x = h(x) \quad p = p(x) \quad (11)$$

Thus, equations (7) through (10) become equations (12) through (15), respectively.

$$f^2 - g^2 + h \, df/dx = \nu \, d^2f/dx^2 \quad (12)$$

$$2fg + h \, dg/dx = \nu \, d^2g/dx^2 \quad (13)$$

$$dh/dx + 2f = 0 \quad (14)$$

$$h \, dh/dx = -1/\rho \, dp/dx - \nu \, d^2h/dx^2 \quad (15)$$

Boundary conditions for the numerical integration are:

$$f(0) = 0 \quad f(\infty) = 0 \quad g(0) = 0 \quad g(\infty) = 0 \quad h(0) = 0$$

After integration the thickness of the boundary layer can be found to be:

$$b = 2.58 \sqrt{(\nu/\omega)} \quad (16)$$

If the gap between the disk and the housing is smaller than the boundary layer, the variation of the tangential velocity across the gap becomes linear in the manner of Couette-flow. Couette-flow is defined as flow between two parallel walls, one of which is at rest, the other moving along its own plane with a constant velocity.

The equation for the shear stress (17) can be solved exactly.

$$\sigma = \mu \, dv/dh \quad (17)$$

with the following boundary equations:

$$\text{for } s = 0 : v = 0$$

$$\text{for } h = s : v = r \, \omega$$

$$\text{so: } \sigma = \mu \, r \, \omega \, s^{-1} \quad (18)$$

The shear stress is a linear function of the radius. A linear velocity profile develops (Figure 2).

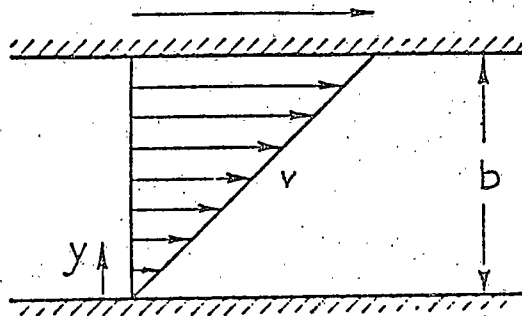


Figure 2. Velocity profile for Couette-flow (Schlichting,1960).

#### Fiber Optic Sensors in Biofilm Research

A literature search was performed to find useful information in previous applications of fiber optic sensing systems for the intended research. Fiber optic sensor technology is a young field; thus only one very recent published book (Krohn, 1988) could be found which encompasses mainly sensor technology. Personick (1985) writes in some detail about sensing systems. A broad range of specialized applications for fiber optic and laser sensors can be found in the proceedings of the meeting of "The International Society for Optical Engineering" (De Paula and Udd, eds.,1987). Especially interesting was one paper by Zhong and Li (1987), which describes the use of an optical fiber sensor for dust concentration measurements. Here absorption of light following the Lambert-Beer Law is used effectively to measure particle concentration. This is similar to our intention to measure the thickness of biofilm.

Two examples for absorption measurements in biofilms were found in the literature. Pedersen (1982a) used the absorbance of stained biofilm to measure biofilm thickness. However, he used a spectrophotometer to measure the absorbance of stained biofilm rather than sensors. The absorbance of biofilm was successfully used to determine its thickness. Jørgensen (1989) measured light penetration and absorption in bacterial mats. He employed a fiber optic microprobe to detect radiance gradients in the bacterial mat. By using the fiber optic microprobe it was possible to measure the spectral quantum flux within small clusters of cells. Quantum flux is the most important light parameter for microbial photosynthesis.

Sensing systems detect physical or chemical conditions and pass this information in suitable form to an operator or to another system or device. A sensing device is composed of four essential components: one or more sensors, processors, an output device and communication links.

A sensor is an input device that transduces a physical or chemical parameter into an electrical or optical signal. A processor converts sensor information into a form suitable for output. An output device presents the processed information to a user, to an actuator or to another system. A communication link provides a path for the transmission of an electrical or optical signal from the sensor to the processor or from the processor to an output device. Typically the path is a wire or optical fiber. The fiber optic sensing device used in this research is assembled in an analogous manner (Figure 3).

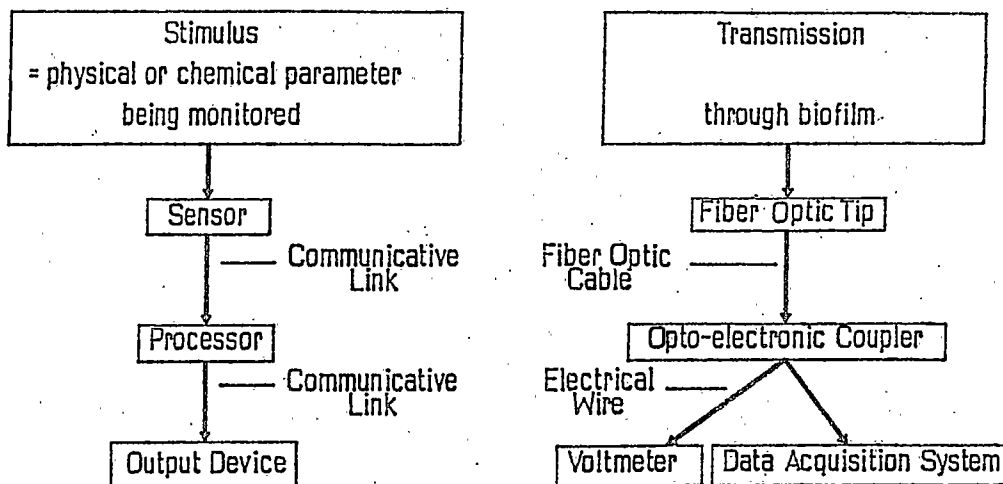


Figure 3. A sensing device in general form and in the form used for the fiber optic sensor.

The sensing device measured light-intensity changes caused by the biofilm. It therefore can be called an intensity-modulated sensor. Intensity-modulated sensors are defined in Krohn (1988) as sensors that detect variations in light intensity. Light intensity variations can be associated with the perturbing environment, i.e., transmission and reflection in biofilm (Figure 4). Intensity-modulated sensors are generally analog devices.

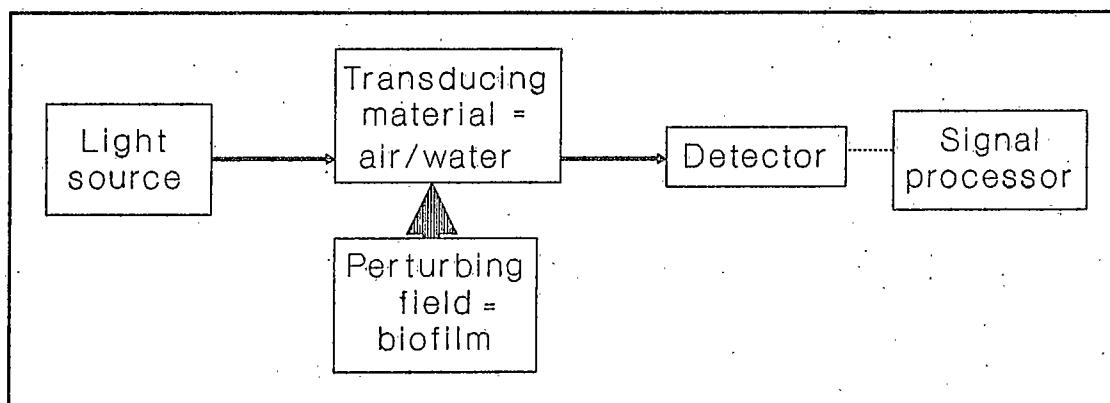


Figure 4: Schematic of an intensity-modulated sensing device.

The light intensity modulation can be described qualitatively by the laws of absorption. Lambert's Law states that the rate of change of light intensity in passing through a homogeneous medium is proportional to the light intensity at any point within that medium, or:

$$dI/dx = -e I, \quad (19)$$

where  $I$  = light intensity

$e$  = extinction coefficient

$x$  = distance

Upon integration, this equation yields:

$$\ln(I/I_0) = -e * d \quad (20)$$

where  $I_0$  is the light intensity at the point where the distance,  $d$ , equals 0. Thus, if the logarithm of light intensity is plotted as a function of distance through a homogeneous medium, a line of constant slope " $e$ " would result. Where the extinction coefficient changes abruptly from one value to another, an abrupt change in the slope of the line would be expected. It is this phenomenon which is to be used to detect the biofilm-water interface. Biofilm has a high extinction coefficient owing to the presence of a variety of light absorbing organic compounds, while the bulk water has a very low extinction coefficient. As the sensor is moved through the bulk water toward the light source, a line of very low slope would be presumed. As the sensor moves through the biofilm, a line of much steeper slope results, corresponding to the extinction coefficient of the biofilm. At the interface between these two media, a distinct break in the slope of the line would be expected.

In a solution, the absorption depends upon the concentration and thickness of the layer traversed. Unit layer and unit concentration absorb equal light as a layer twice

as thick but with half the concentration. Calling the absorption coefficient of unit concentration  $\epsilon$ , the thickness  $d$  and the concentration  $c$ , we have:

$$I = I_0 * e^{-\epsilon cd} \quad (\text{Beer's Law}), \text{ or} \quad (21)$$

$$\ln(I_0/I) = \epsilon cd \quad (22)$$

The  $\ln(I_0/I)$  is called absorbance. Beer's Law states that absorbance is linearly proportional to concentration. Thus, a relationship between the biofilm density and the slope of the absorbance curve is expected.

The changes in light intensity, caused by absorption, were registered with a fiber optic sensor. Extrinsic and intrinsic capabilities of the sensor were used to determine biofilm thickness. Extrinsic fiber optic sensors use the optical fiber as a transmission line to convey modulation of light intensity. In intrinsic sensors the optical fiber changes physically in response to the physical or chemical parameter being monitored. A physical change of the fiber is bending of the fiber, which occurs as a response to touching of the substratum surface. The optical principles of refraction and reflection describe the detection of light with a fiber optic sensor.

Refraction occurs when light passes from one homogenous isotropic medium to another. In our case the two media considered are air and the glass of the optic cable. The light ray will bend at the interface between the two media. The mathematic expression that describes the refraction phenomena is known as Snell's Law, which can be derived from Maxwell's Equations.

$$n_0 \sin \alpha_0 = n_1 \sin \alpha_1 \quad (\text{Snell's Law}) \quad (23)$$

where  $n_0$  = the index of refraction of the medium in which the light is initially travelling

$n_1$  = the index of refraction of the second medium

$\alpha_0$  = the angle between incident ray and the normal to the interface

$\alpha_1 =$  the angle between refracted ray and the normal to the interface

In the case of light passing from a high index medium to a low index medium refraction is occurring, but a certain portion of the incident ray is reflected.

The transmission of the light ray through the fiber optic cable is explained by total internal reflection. If the incident ray hits the boundary at ever increasing angles, a value of  $\alpha_0 = \alpha_c$  will be reached at which no refraction will occur. The angle,  $\alpha_c$ , is called the critical angle. The refracted ray propagates along the interface, not penetrating the lower index medium. So  $\alpha_1 = 90^\circ$  and therefore,  $\sin \alpha_c = n_1/n_0$ . For incident angles greater than the critical angle the ray is entirely reflected at the interface and no refraction takes place. This phenomena is known as total internal reflection.

In Figure 5 the refraction of the ray can be seen as it enters a flat-ended fiber cable. Total internal reflection can be observed as the ray propagates along the cylinder of the cable.

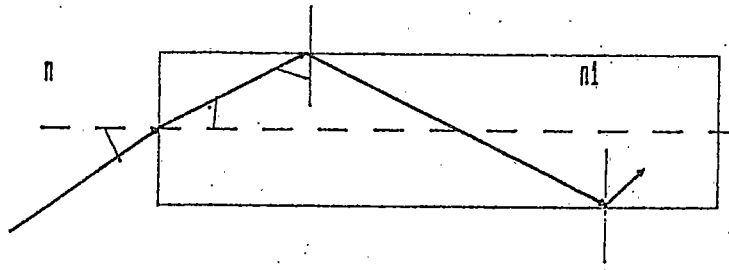


Figure 5. Path of a ray through a fiber optic cable.

The fiber bends when it touches the surface of the substratum. This can be detected, because the ray propagation is disturbed in a curved fiber. For a straight fiber, the angle between the light ray and the normal to the plane of reflection is defined by the angle  $\phi$ . However, when the fiber is bent, the plane of reflection and the reflective angle

rotate by the angle  $\delta$  (Figure 6). Therefore, for a curved fiber, the angle between the reflected and the tangent at the reflection point is  $\phi - \delta$ . In a straight fiber, for  $\phi > \phi_c$ , the rays will be totally internally reflected. In a bent fiber the effective critical angle is reduced by  $\delta$ . Therefore, rays incident between  $\phi_c$  and  $\phi_c - \delta$  will be lost. The effective critical angle is reduced in a bent fiber, and the amount of light that can be detected at the end of the fiber is reduced.

A second mechanism adds to decrease the amount of transmitted light further. In this study the light source was in direct line with the sensor. When the sensor is moved into a hard surface, it not only starts bending, but the sensor tip will also move sideways. Thus, the sensor is not pointed in the direction of the light source anymore and the possible light uptake is decreased. Both effects are responsible for a decrease in registered light intensity.

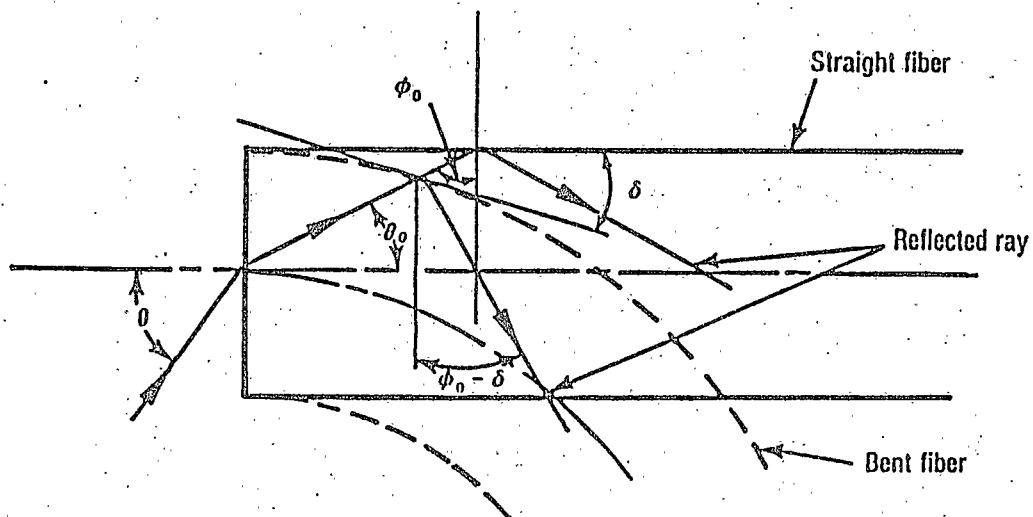


Figure 6. Bending effects on critical angle (Krohn, 1988).

Ambient light was prevented from interfering with the measurements through frequency modulation. The light source was frequency modulated with a frequency of

1000 Hz. Modulation is a systematic alteration of the wave which carries the message. An illustration of frequency modulation can be seen in Figure 7. In analog modulation the modulated parameter varies in direct proportion to the modulating signal. Modulation is a reversible process, so the message can be retrieved at the receiver by the complementary operation of demodulation, where unmodulated light signals are discarded. Thus, ambient light is filtered out.

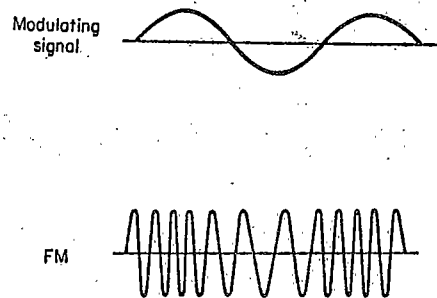


Figure 7. Frequency modulation with a sinusoidal modulating wave. The detector and the light source are modulated at the same frequency, eliminating the effects of ambient light on the measurement.

The optical signal produced with the fiber optic sensor had to be converted to an electrical signal to allow easy recording of the measured data. The device which converts the optical signal into a voltage or current is called the optical detector. A detector with its interfacing electronic circuit is called a receiver. In this experiment, the light intensity is converted into a voltage signal.

The approach to implementing an optical detector is to allow the incident power to illuminate a semiconductor device, resulting in the generation of hole-electron pairs by

absorbed photons. These pairs can in turn flow in the presence of an electric field to produce an observable current. The current can be measured, or else the corresponding potential.

## MATERIALS AND METHODS

The experimental setup and the procedures used for the research are described in the following sections.

### The Rotating Disk Reactor

A mixed population biofilm was grown in a rotating disk reactor (Figure 8). The reactor vessel was a square container made out of transparent polycarbonate with a side length of 70 cm and a reactor height of 20 cm. A disk with a radius of 30 cm rotated in the reactor. Radial grooves were cut into the lower side of the disk, where transparent polycarbonate slides could be inserted. The disk rotated at a distance,  $s$ , of 2 mm from the bottom of the vessel and was submerged 5 cm. An electrical motor was used to turn the disk at a rotational speed,  $\omega$ , of  $1.05 \text{ s}^{-1}$ . An electric thermostat held the water temperature constant at  $20^\circ\text{C}$ , resulting in an absolute viscosity of  $0.01 \text{ g cm}^{-1} \text{ sec}^{-1}$  and a kinematic viscosity of  $1.01 \cdot 10^{-6} \text{ m}^2 \text{ s}^{-1}$ . The Reynolds number for this condition is  $9 \cdot 10^4$ , which indicates laminar flow and a boundary layer thickness of 2.5 mm. Thus, a linear velocity distribution existed in the reactor; the conditions for laminar Couette-flow were met, and the shear stress could be calculated.























































































































































































